Supplemental Data

Figure S1. Histological analysis of postnatal myometrial defects in *Tgfbr1* cKO mice. (A-J) PAS-hematoxylin staining of uterine sections at P0 (A and B), P3 (C and D), P5 (E and F), P10 (G and H), and P15 (I and J) from control and *Tgfbr1* cKO mice. Representative images are shown for each time point (*n* = 3). Red dotted lines indicate the circular smooth muscle layers in the control mice. Note the formation of circular myometrium in the controls during P3-P15, and the disorganized smooth muscle in the *Tgfbr1* cKO mice. CM, circular smooth muscle layer; Ep, epithelium. Scale bar = 20 μm.

Figure S2. Uterine adenomyosis in *Tgfbr1* cKO mice. (A-D) Immunofluorescence of ACTA2 (Red) in the uteri of a 3-month old control (A and C) and *Tgfbr1* cKO mice (B and D). CM, circular smooth muscle layer; LM, longitudinal smooth muscle layer. (E and F) Immunohistochemical staining of CNN1 (brown staining) in the uteri of 3-month old control (E) and *Tgfbr1* cKO mice (F). The sections were counter stained with hematoxylin. Representative images are shown for each group (*n* = 3). Note the disrupted myometrium and presence of uterine glands (denoted by *) within the myometrium of *Tgfbr1* cKO mice compared with controls in which highly organized myometrium was visualized. Scale bar = 50 μm.

Figure S3. Expression and localization of FN1 in the uteri of control and *Tgfbr1* cKO

mice. (A) Transcript levels of *Fn1* in wild type uterus during postnatal uterine development at P0 (*n* = 5), P3 (*n* = 4), P5 (*n* = 3), P10 (*n* = 4), and P15 (*n* = 4). (B) Relative levels of mRNA for *Fn1* in the uterus of control and *Tgfbr1* cKO mice at P5 (*n* = 5 per group). Data are mean ± SEM. NS, no significance. (C-F) Immunofluorescence of FN1 (green) and ACTA2 (red) in the uteri of control (C and D) and *Tgfbr1* cKO (E and F) mice. CM, circular smooth muscle layer; Ep, epithelium. Scale bar = 20 μm.

Figure S4. Abnormal distribution of vasculature in *Tgfbr1* cKO uterus at P15. (A and B) Double immunofluorescence of CD31 (Red) and ACTA2 (Green) without (A) or with DAPI (Blue; B). Note that vessels were well organized and mostly distributed between circular and longitudinal muscle layers and within the endometrium on the cross section. (C-F) Double immunofluorescence of CD31 (Red) and ACTA2 (Green) without (C and E) or with DAPI (Blue; D and F). Arrows indicate uterine vessels. Note the presence of vessels inside the disrupted myometrial layers of the *Tgfbr1* cKO uteri. (G and H) Representative negative controls where primary antibodies were replaced with rabbit (G) or mouse (H) IgG. Note no specific staining was detected in the absence of primary antibodies. CM, circular smooth muscle layer; LM, longitudinal smooth muscle layer. Scale bar (20 μm) is representatively depicted in (A).

Figure S5. Impaired laminin production by myometrial cells during early uterine development. (A-F) Subcellular localization of laminin (Green; A and B), ACTA2 (Red; C

and D), and laminin and ACTA2 (E and F) in the uteri of control mice at P5. (G-L) Subcellular localization of laminin (Green; G and H), ACTA2 (Red; I and J), and laminin and ACTA2 (K and L) in the uteri of *Tgfbr1* cKO mice at P5. Note the lack of typical laminin immunofluorescence signals in the smooth muscle cells of *Tgfbr1* cKO mice (G-L) compared with controls (A-F). Representative images are shown for each group (*n* = 3). The yellow dotted lines indicate the circular smooth muscle layers developed at P5. CM, circular smooth muscle layer; LAM, laminin. Scale bar = 20 μm.

Figure S1

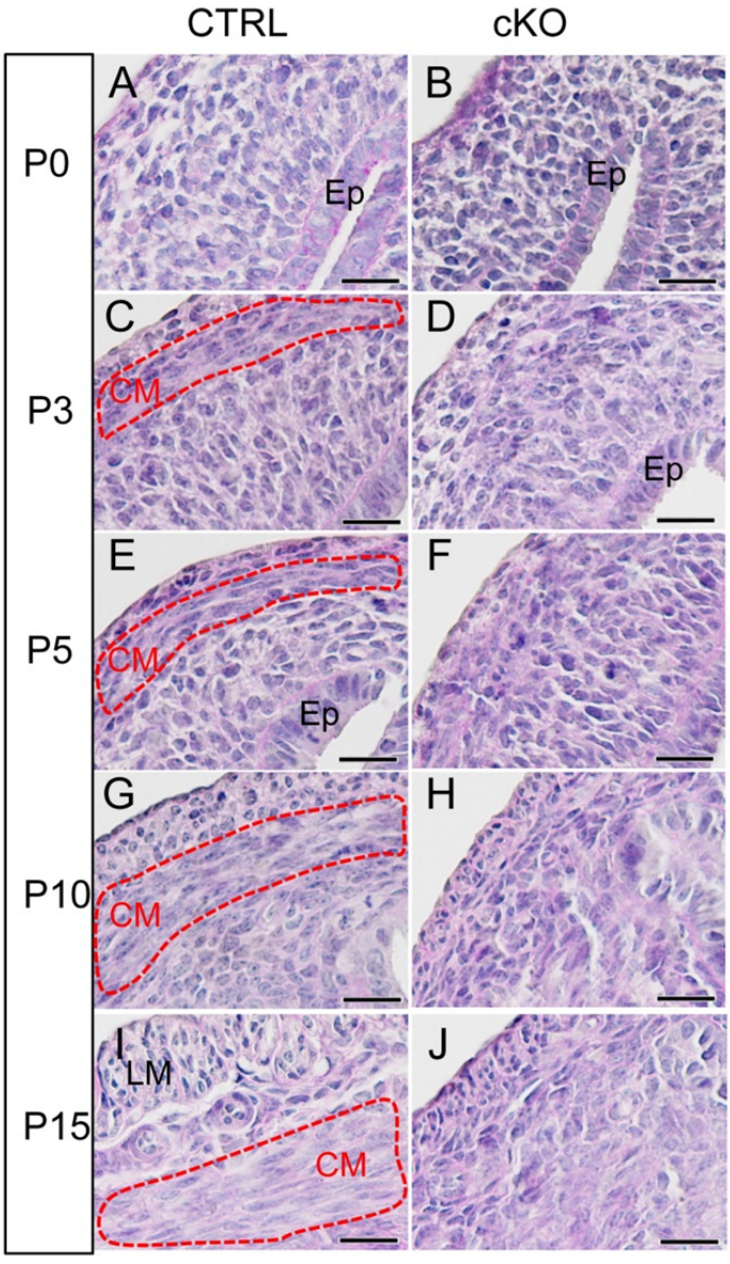

Figure S2

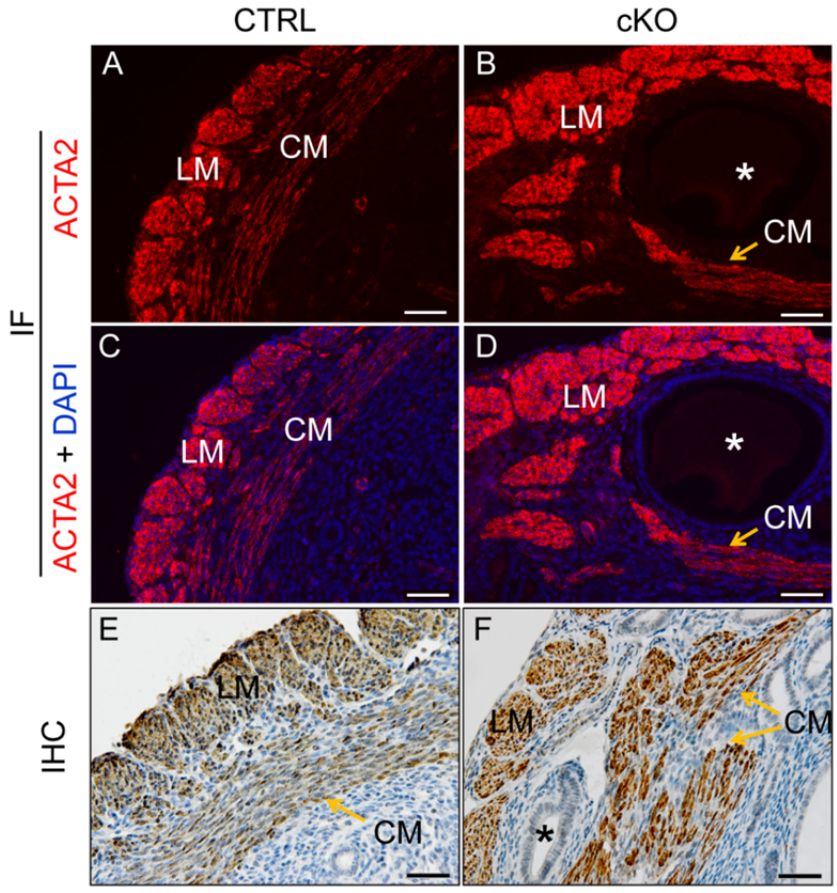

Figure S3

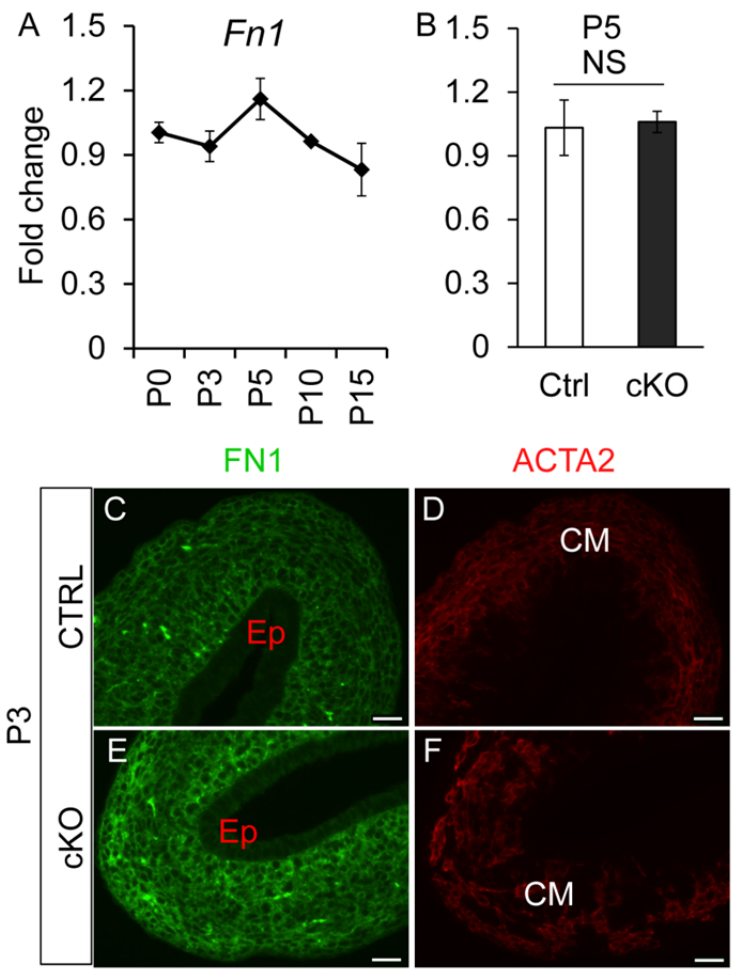
A
Fn1
Fold change
1.5
1.2
0.9
0.6
0.3
0
P0
P3
P5
P10
P15
B
P5
NS
Ctrl
cKO
FN1
ACTA2
P3
CTRL
cKO
C
D
E
F
Ep
Ep
CM
CM

Figure S4

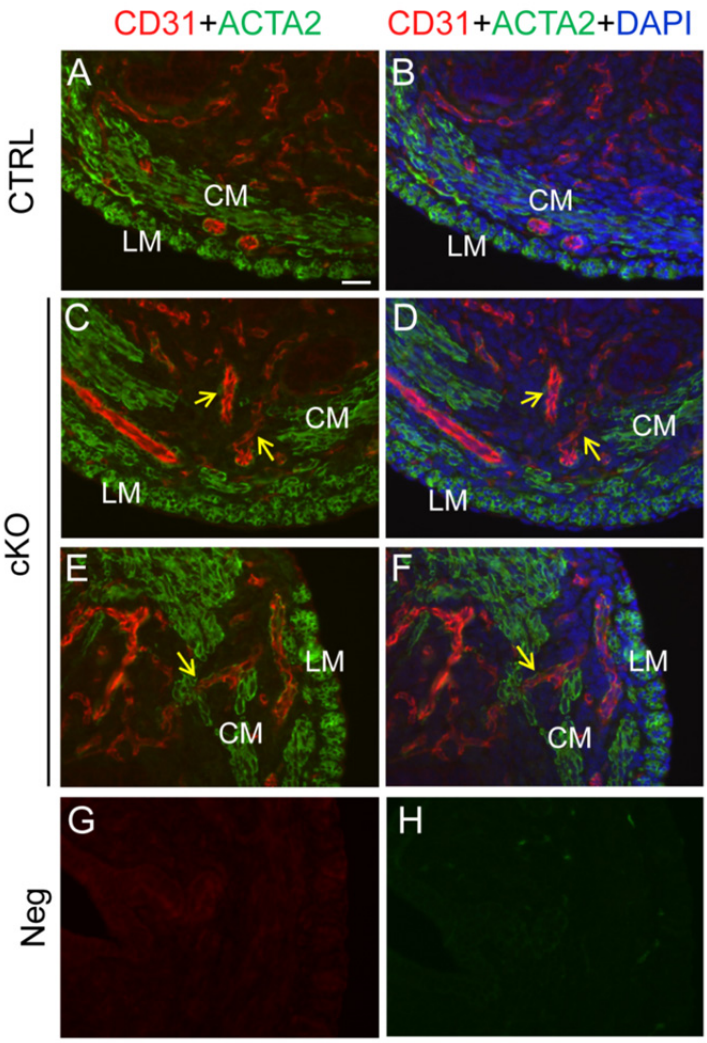

Figure S5

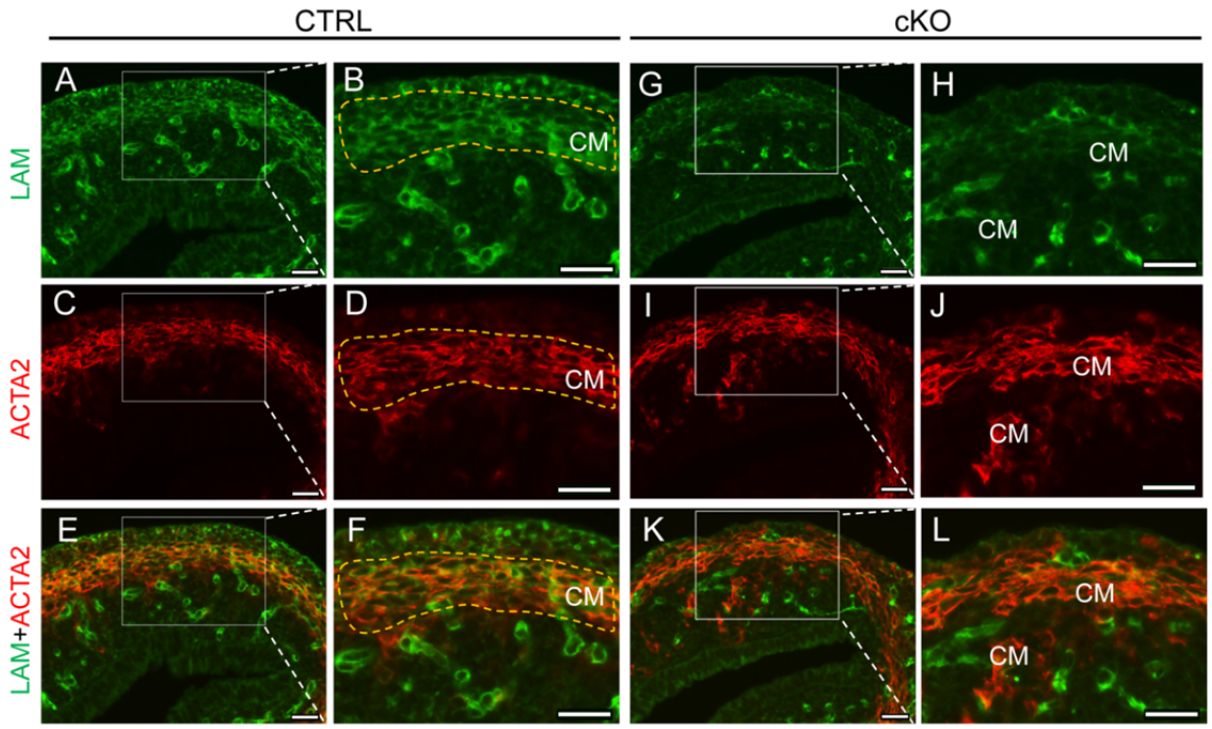
CTRL
cKO
LAM
ACTA2
LAM+ACTA2
A
B
C
D
E
F
G
H
I
J
K
L
CM
CM
CM
CM
CM
CM
CM
CM
CM
CM
CM
CM